PADOVA UNIVERSITY PRESS

Dolomites Research Notes on Approximation

Volume 12 · 2019 · Pages 86–100

Smoothing exponential-polynomial splines for multiexponential decay data

Rosanna Campagna [a] · Costanza Conti [b] · Salvatore Cuomo [c]

Communicated by Len Bos

Abstract

In many applications, the definition of fitting models that mimic the behaviour of experimental data is a challenging issue. In this paper a data-driven approach to represent (multi)exponential decay data is presented. We propose a fitting model based on smoothing splines defined by means of a differential operator. To solve the linear system involved in the smoothing exponential-polynomial spline definition, the main idea is to define *B-spline like* functions for the spline space, that are locally represented by *Bernstein-like bases* through Hermite interpolation conditions.

1 Introduction

Several engineering and life science applications require the use of fitting/interpolating models to represent experimental data. A functional description of such information gives the possibility of adopting powerful mathematical tools for data analysis such as the Fourier/Laplace transforms or the integro-differential approaches. An extensive literature indicates splines as very interesting functional models to analyse and represent data in several research fields. For example, in EEG functions (see [1]), a Laplacian estimator based on a tensorial formulation of the surface based on thin plate spline functions to describe a realistic scalp surface has been presented. In [2], a medical application based on biomarkers is presented; a longitudinal and survival fitting model based on cubic polynomial B-splines sets is presented for modeling the longitudinal markers. A spatial interpolation functional approach to represent large climate data set, based on bivariate thin plate smoothing splines, has been presented in [3]. Moreover, the paper [4] describes the analysis of fluorescence depolarization data in membrane vesicles using exponential spline interpolating functions.
In this work, we are interested in the modelling of data with exponential decay. A well-known example of this context is the *NMR data analysis* where the magnetization *decays* as a function of time and, generally, the NMR relaxation signal, s, is the sum of exponentially decaying components, depending on *relaxation times*, T_j:

$$s(t) = \sum_{j=1}^{M} p_j e^{-t/T_j},$$

where t is the experimental time, M is the number of micro-domains having the same spin density p_j and the same relaxation time T_j. >From a mathematical point of view, sometimes it is very useful to represent the relationship between the NMR relaxation signal s and the corresponding distribution function G of the relaxation times by means of an integral function, e.g. due to the extreme complexity of heterogeneous systems [5]:

$$s(t) = \int_0^{+\infty} G(T) e^{-t/T} dT.$$

The Laplace transform (LT) inversion methods are usually adopted for computing the inversion recovery. Unfortunately they require information on the LT function that are often unknown [6], [7], [8]. To overcome this issue, general-purpose software packages (e.g. [9]) are used for the LT inversion (see [10], [11] and the web page [12]).

Behaviors in NMR, modelled by LT, can give exponential decay samples. The main contribution of this paper is to define and construct a *spline model* on suitable function spaces that are able to reproduce this kind of data. In a previous paper [13] there was defined a *smoothing spline* on $[x_1, +\infty)$ piecewise defined like a polynomial complete smoothing spline of 4th order between the knots $[x_1, x_n]$ and an exponential-polynomial model in the span$\{x^{\theta_1} e^{\theta_2 x}\}$, with $\theta_1, \theta_2 \in \mathbb{R}$, outside the knots, in $[x_n, +\infty)$; moreover, the model enjoys second order regularity, $C^2(x_1, x_n)$ and it is continuous up to *only the first* derivative at x_n.
Here we propose a *natural smoothing exponential-polynomial spline*, defined through local bases enjoying several properties of

[a] Department of Agricultural Sciences, University of Naples Federico II, Italy
[b] Department of Industrial Engineering, University of Florence, Italy
[c] Department of Mathematics and Applications "R. Caccioppoli", University of Naples Federico II, Italy

polynomial B-splines, called *B-spline like* or *generalized B-splines* (GB-splines), with higher regularity between the knots, at least C^2 in a wider interval, $[a, b]$, including the knots. Firstly, we define the differential operator and the corresponding null space characterizing the natural smoothing spline. Using classical results form the theory of L-smoothing splines (see [14] and [15]) we know that the smoothing spline coefficients are given by the solution of a linear system whose conditioning depends on the bases used to express the spline. Hence, our idea is to follow [16] and [17] (see also [18] in the cardinal situation) and define suitable GB-bases with pieces expressed in terms of proper Bernstein(-like) local bases; regularity conditions are also imposed in order to make the GB-splines globally C^2. A Bernstein basis is more handy than the canonical one (standard exponential-polynomials) in particular when imposing Hermite conditions at internal nodes. The natural smoothing exponential-polynomial spline we derive this way fits the data as expected.

In Section 2 we firstly define some mathematical preliminaries on the L-spline definition model. Section 3 gives the definition of the GB-splines, based on results about the Bernstein(-like) bases recalled in the Appendix A, and a constructive algorithm for the smoothing spline. Numerical results are discussed in Section 4. The last section deals with conclusions and future work.

2 Mathematical preliminaries and model definition

We recall the main notations and definitions starting from [15] even though many other papers or books can be used to start with such as, e.g. [19].

Firstly we set a space on which we define the fitting model as a natural L-spline.

Definition 2.1. For a given partition of the interval $[a, b]$, $\Delta := \{a < x_1 < \dots x_N < b\}$, set the space:

$$H^n[a, b] := \{u \in C^{n-1}[a, b],\ u^{(n-1)} \text{ abs. cont. in } [a, b],\ \text{and } u^{(n)} \in L^2[a, b]\}.$$

The *natural* L-spline related to a differential operator $\mathcal{L}_n$, of order n, defined on Δ, is a function $s \in H^n[a, b]$ such that:

- $s \in H^{2n-1}[a, b]$;
- $\mathcal{L}_n^* \mathcal{L}_n s = 0$ in every interval (x_i, x_{i+1}), $i = 1, \cdots, N-1$;
- $\mathcal{L}_n s = 0$ in $(a, x_1) \cup (x_N, b)$ (*natural* end conditions).

Particularly, the *smoothing* natural L−spline can be defined by solving a minimization problem as in the following.

Definition 2.2. Given a partition of the interval $[a, b]$, $\Delta := \{a < x_1 < \dots x_N < b\}$, a vector $(y_1, \cdots, y_N) \in \mathbb{R}^N$, and the *natural* L-spline in Definition 2.1, a *natural smoothing* L*−spline*, related to a fixed differential operator $\mathcal{L}_n$ of order n, on the partition Δ of $[a, b]$, is the solution of the problem

$$\min \quad \left\{ \sum_{i=1}^{N} (w_i[u(x_i) - y_i]^2 + \lambda \int_a^b (\mathcal{L}_n u(x))^2\, dx \right\}, \quad u \in H^n[a, b]. \tag{1}$$

with $(w_1, \dots, w_N)$ non zero weights and λ is a regularization parameter.

The existence and uniqueness of this fitting model has been proved in [15] where the notion of Chebyshev system is defined and used:

Theorem 2.1. *If the null space of $\mathcal{L}_n$ is a Chebyshev system, then the natural L-smoothing spline is the* unique *solution of* (1) *in the form:*

$$s(x) = \sum_{i=1}^{N} c_j \varphi_j(x), \tag{2}$$

where $\varphi_1, \cdots \varphi_N$ are basis functions and the coefficient vector $c = (c_1, \cdots, c_N)$ is the solution of the linear system:

$$(\Phi + (-1)^n \lambda W\, D)\, c = y, \tag{3}$$

where the $N \times N$ matrices Φ and D are

$$\Phi = (\varphi_j(x_i))_{i,j=1}^N, \quad D = (\varphi_j^{(2n-1)}(x_i^+) - \varphi_j^{(2n-1)}(x_i^-))_{i,j=1}^N.$$

and $W := diag(1/w_1, \cdots, 1/w_N)$ is a nonsingular diagonal matrix.

It is obvious that the conditioning of the linear system (3) depends on the basis used to define the spline and the construction of a *local* basis will play an important role.

We start by defining a differential operator $\mathcal{L}_2$, then the related L−spline functions space and, finally, the basis $(\varphi_j)_{j=1,\dots,N}$. Let $n = 2$, so that our $2nd$ order differential operator is

$$\mathcal{L}_2 u := u'' + 2\alpha u' + \alpha^2 u, \quad u \in H^2[a, b], \quad \alpha \in \mathbb{R}^+, \tag{4}$$

its adjoint has the form

$$\mathcal{L}_2^* v = v'' - 2\alpha v' + \alpha^2 v, \quad v \in H^2[a,b], \quad \alpha \in \mathbb{R}^+ \tag{5}$$

and the $4th$ order differential operator is:

$$\mathcal{L}_2^* \mathcal{L}_2 v = v^{(iv)} - 2\alpha^2 v'' + \alpha^4 v, \quad v \in H^4[a,b], \quad \alpha \in \mathbb{R}^+. \tag{6}$$

The corresponding null spaces of $\mathcal{L}_2$ and $\mathcal{L}_2^* \mathcal{L}_2$ are, respectively, the following two and four dimensional spaces:

$$\mathbb{E}_2 := \text{span}\{e^{-\alpha x},\ x\, e^{-\alpha x}\}, \quad \alpha \in \mathbb{R}^+,$$

and

$$\mathbb{E}_4 := \text{span}\{e^{\alpha x},\ x\, e^{\alpha x},\ e^{-\alpha x},\ x\, e^{-\alpha x}\}, \quad \alpha \in \mathbb{R}^+.$$

We highlight that the two spaces $\mathbb{E}_2$, $\mathbb{E}_4$ are Chebyshev on the real line spanned by linear independent functions.

We search for a model spline space defined in the following:

Definition 2.3. The spline space $S_{\mathcal{L}_2,\Delta}$ contains the natural $L-$splines, related to $\mathcal{L}_2$ on Δ, such that:

(a) $s \in H^3[a,b]$;
(b) $\mathcal{L}_2^* \mathcal{L}_2 s = 0$ in every interval (x_i, x_{i+1}), $i = 1, \cdots, N-1$;
(c) $\mathcal{L}_2 s = 0$ in $(a, x_1) \cup (x_N, b)$.

$S_{\mathcal{L}_2,\Delta}$ is a N dimensional vector space. Indeed, any $s \in S_{\mathcal{L}_2,\Delta}$ presents $4(N-1) + 2 \cdot 2$ degrees of freedom (d.o.f.), due to $(N-1)$ pieces belonging to a 4-dimensional space, and 2 pieces in a 2-dimensional space; moreover $3N$ conditions derive from the C^2-continuity at x_i, $i = 1, \ldots, N$.

For simplicity of notation, from now on we omit the subscript related to the differential order in the space name.

3 Computation of the GB-spline basis functions

The construction of a *local* basis for $S_{\mathcal{L},\Delta}$ is the main goal of this section. More in detail, following the formulation of the *polynomial* B-splines, our problem consists in setting the basis functions $\varphi_j \in S_{\mathcal{L},\Delta}$ for $j = 1, \cdots, N$, satisfying

(a*) the support of each φ_j is compact;
(b*) $\varphi_j \in C^2[a,b]$;
(c*) $\varphi_j \in \mathbb{E}_4$ for $x \in (x_i, x_{i+1})$, $i = 1 \cdots, N-1$;
(d*) $\varphi_j \in \mathbb{E}_2$ for $x \in (a, x_1)$ or $x \in (x_N, b)$;
(e*) φ_j, $j = 1, \ldots, N$, are positive and *bell shaped* functions.

Note that condition (a^*) grants a banded linear system (3); conditions (c^*) and (d^*) characterize *boundary* and *regular*, or internal, GB-splines respectively. The former are 4 functions, denoted by N_ℓ^4, $\ell = 1, 2, N-1, N$, C^2-continuous in (a,b), are piecewise defined with segments in $\mathbb{E}_2$ in the part of their support outside of the knots interval $I = [x_1, x_N]$ and segments in $\mathbb{E}_4$ in the part of their support inside I. Their support is assumed to be $[x_{\ell-2}, x_{\ell+2}]$, $\ell = 1, 2, N-1, N$ where $x_{-1} < a = x_0$ and $x_{N+2} > x_{N+1} = b > x_N$. The regular basis functions, denoted by N_ℓ^4, $\ell = 3, \cdots, N-2$, are C^2-continuous piecewise defined functions with all segments in $\mathbb{E}_4$ and with the support assumed to be $[x_{\ell-2}, x_{\ell+2}]$, $\ell = 3, \ldots, N-2$.

Regarding the boundary functions, we point out that we extend the approach in [17] where only Chebyshev spaces with the same dimension are discussed. Moreover, we highlight that for their construction, some additional knots have to be considered on each side outside of I, more in detail *two* on the left of x_1 (labelled as x_{-1}, x_0) and *two* on the right of x_N (labelled as x_{N+1}, x_{N+2}).

3.1 Construction of the regular bases

A constructive strategy to define the N_ℓ^4, $\ell = 3, \cdots, N-2$ is to write them in each interval $[x_j, x_{j+1}]$, $j = \ell-2, \cdots, \ell+1$, in terms of the *Bernstein-like basis functions* of $\mathbb{E}_4$ (see Appendix), to impose interpolating conditions (zero interpolation up to order 2) at the boundary points $x_{\ell-2}$ and $x_{\ell+2}$ and finally to impose C^0, C^1, C^2 regularity between each piece at the internal points $x_{\ell-1}$, x_ℓ, $x_{\ell+1}$. In other words, each function will be written as

$$N_\ell^4(x)|_{[x_j, x_{j+1}]} = \sum_{i=0}^{3} \gamma_{\ell,j,i} \tilde{B}_i(x - x_j), \quad j = \ell-2, \cdots, \ell+1,$$

where $\tilde{B}_i(x - x_j)$, $i = 0, \cdots, 3$ are the four Bernstein like functions related to $[x_j, x_{j+1}]$. It means that N_ℓ^4 will be identified by 16 coefficients $\gamma_{\ell,j,i}$, $i = 0, \cdots, 3$, $j = \ell-2, \cdots, \ell+1$. The advantage of using a Bernstein type representation of the pieces is that, regularity and boundary interpolation translates into 15 relatively simple conditions. The main drawback in this approach is that these 15 relatively simple conditions *do not uniquely* identify N_ℓ^4 and no positivity is guaranteed.

As an alternative, to uniquely identify N_ℓ^4, following [17] we introduce the Bernstein-like bases for the bigger space $\mathbb{E}_5 :=$ *span*$\{1, e^{\alpha x},\ x\, e^{\alpha x},\ e^{-\alpha x},\ x\, e^{-\alpha x}\}$, based on which we construct the piecewise defined function M_ℓ with breakpoints $x_{\ell-2}, \cdots, x_{\ell+2}$. A crucial point here is that $\mathbb{E}_5' := \mathbb{E}_4$ so $\mathbb{E}_5$ is actually an extended Chebyshev space [21].

Proposition 3.1. *The regular GB-splines* $N_\ell^4(x)$, $\ell = 3, \ldots, N-2$ *are uniquely defined as*

$$N_\ell^4 = (M_\ell)', \quad \ell = 3, \ldots, N-2$$

with M_ℓ *the piecewise defined function satisfying*

(i) $M_\ell(x)|_{[x_j, x_{j+1}]} = \sum_{i=0}^4 \beta_{\ell,j,i} B_i^5(x - x_j)$, $j = \ell-2, \cdots, \ell+1$ *with* B_i^5, $i = 0, \ldots, 4$ *Bernstein-like basis functions of* $\mathbb{E}_5$ *related to* $[x_j, x_{j+1}]$*;*

(ii) M_ℓ *and* $1 - M_\ell$ *vanish, together with their derivatives, up to order three, at* $x_{\ell-2}$ *and* $x_{\ell+2}$*, respectively;*

(iii) the M_ℓ *are* C^3*-regular at the internal points* $x_{\ell-1}$, x_ℓ, $x_{\ell+1}$.

Proof. >From (i), each M_ℓ has 20 d.o.f.; moreover (ii) and (iii) translate in 8 and 12 conditions respectively, so the functions M_ℓ are uniquely given by a non-singular square linear system and, as a consequence, also the GB-splines N_ℓ^4. Such linear system is certainly non-singular since it is proven in [21] that the piecewise Chebyshevian spline space with segments in E_5 is *good for design*, meaning that they possess a B-spline basis. Therefore, non-singularity is guaranted. We continue by explaining the linear system to be solved to get the functions M_ℓ denoting, for simplicity, $M_\ell^j = M_\ell(x)|_{[x_j, x_{j+1}]}$ and

$$(M_\ell^j)^{(k)}(x) = \sum_{i=0}^{4} \beta_{\ell,j,i} (B_i^5(x - x_j))^{(k)}, \quad k = 0, \ldots, 3. \tag{7}$$

From (ii):

$$(M_\ell^{\ell-2})^{(k)}(x_{\ell-2}) = 0, \quad k = 0, \cdots, 3 \quad \Leftrightarrow \beta_{\ell,\ell-2,k} = 0, \quad k = 0, \cdots, 3, \tag{8}$$

and

$$(1 - M_\ell^{\ell+1})^{(k)}(x_{\ell+2}) = 0, \quad k = 0, \cdots, 3 \quad \Leftrightarrow \beta_{\ell,\ell+1,4-k} = 1, \quad k = 0, \cdots, 3. \tag{9}$$

Concerning (iii) let us start by considering the point $x_{\ell-1}$ and write the condition for C^k-regularity for $k = 0, \cdots, 3$ that is

$$(M_\ell^{\ell-2})^{(k)}(x_{\ell-1}) = (M_\ell^{\ell-1})^{(k)}(x_{\ell-1}), \quad k = 0, \cdots, 3.$$

The previous conditions translate into 4 linear equations. Analogously, imposing regularity at x_ℓ,

$$(M_\ell^{\ell-1})^{(k)}(x_\ell) = (M_\ell^{\ell})^{(k)}(x_\ell), \ k = 0, \cdots, 3.$$

Finally, imposing regularity at $x_{\ell+1}$, that is

$$(M_\ell^{\ell})^{(k)}(x_{\ell+1}) = (M_\ell^{\ell+1})^{(k)}(x_{\ell+1}), \ k = 0, \cdots, 3,$$

we get the last 4 equations. Taking into account equations (8) and (9), the 20 equations can be reduced to 12, that uniquely identify the coefficients vector

$$(\beta_{\ell,\ell-2,4}, \beta_{\ell,\ell-1,0}, \cdots, \beta_{\ell,\ell-1,4}, \beta_{\ell,\ell,0}, \cdots, \beta_{\ell,\ell,4}, \beta_{\ell,\ell+1,0})^T \ \in \mathbb{R}^{12\times 1} \tag{10}$$

and so the function M_ℓ piecewise defined as in (i). □

In Fig. 1 is described the behaviour of a generic M_ℓ and the corresponding regular N_ℓ, for a particular choice of $\alpha = 1/2$.

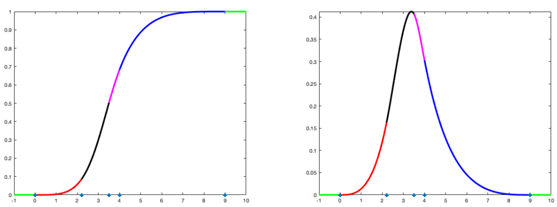

Figure 1: Function M_ℓ (left) and corresponding N_ℓ (right) for $\alpha = \frac{1}{2}$ and knots denoted by $'*'$.

3.2 Construction of the left boundary bases

Similarly to the previous section, we construct N_1^4 supported on $[x_{-1}, x_3]$, with $x_{-1} < a,\ x_0 = a$. Then, we construct N_2^4, supported on $[x_0, x_4]$. They are defined by using the *extended Chebyshev space* $\mathbb{E}_3 := span\{1, e^{-\alpha x},\ x\,e^{-\alpha x}\}$, such that $\mathbb{E}_3^{'} \equiv \mathbb{E}_2$.

Proposition 3.2. *The boundary function N_1^4 is uniquely identified as $N_1^4 = (M_1)^{'}$ with M_1 the piecewise defined function satisfying*

(i) $M_1(x)|_{[x_j, x_{j+1}]} = \sum_{i=0}^{2} \beta_{1,j,i} B_i^3(x - x_j)$, $\ j = -1, 0$ *while* $M_1(x)|_{[x_j, x_{j+1}]} = \sum_{i=0}^{4} \beta_{1,j,i} B_i^5(x - x_j)$, $\quad j = 1, 2$;

(ii) *M_1 and $1 - M_1$ vanish together with their first derivatives at x_{-1} and with their derivatives up to the third order at x_3, respectively;*

(iii) *is C^1-regular at x_0 and C^3-regular at the internal knots $x_1,\ x_2$.*

Proof. Once again, since the number of d.o.f. coincides with the number of conditions, the function M_1 is uniquely determined by a square linear system, and so is N_1^4. To obtain the explicit expression of M_1 we need to solve a linear system whose equations are coming next with the shorthand notation $M_1^j = M_1(x)|_{[x_j, x_{j+1}]},\ j = -1, \cdots, 2$. Indeed, (ii) translates into:

$$(M_1^{-1})^{(k)}(x_{-1}) = 0, \quad k = 0, 1 \quad \Leftrightarrow \beta_{1,-1,k} = 0, \quad k = 0, 1, \tag{11}$$

and

$$(1 - M_1^2)^{(k)}(x_3) = 0, \quad k = 0, \cdots, 3 \quad \Leftrightarrow \beta_{1,2,4-k} = 1, \quad k = 0, \cdots, 3. \tag{12}$$

Concerning (iii), at the point x_0 we get

$$(M_1^{-1})^{(k)}(x_0) = (M_1^0)^{(k)}(x_0), \quad k = 0, 1,$$

that in terms of Bernstein functions is:

$$\sum_{i=0}^{2} \beta_{1,-1,i} (B_i^3)^{(k)}(h) = \sum_{i=0}^{2} \beta_{1,0,i} (B_i^3)^{(k)}(0). \tag{13}$$

Regularity at x_1 and x_2 reads as

$$(M_1^{\ell})^{(k)}(x_{\ell+1}) = (M_1^{\ell+1})^{(k)}(x_{\ell+1}), \quad k = 0, \cdots, 3, \quad \ell = 0, 1,$$

translating into the linear equations ($\ell = 0$):

$$\sum_{i=0}^{2} \beta_{1,0,i} (B_i^3)^{(k)}(h) = \sum_{i=0}^{4} \beta_{1,1,i} (B_i^5)^{(k)}(0), \tag{14}$$

and similarly ($\ell = 1$):

$$\sum_{i=0}^{4} \beta_{1,1,i} (B_i^5)^{(k)}(h) = \sum_{i=0}^{4} \beta_{1,2,i} (B_i^5)^{(k)}(0). \tag{15}$$

Taking into account equations (11) and (12), the 16 equations can be reduced to 10, that, according with the arguments of Proposition 3.1, uniquely identify the coefficients vector

$$(\beta_{1,-1,2}, \beta_{1,0,0}, \cdots, \beta_{1,0,2}, \beta_{1,1,0}, \cdots, \beta_{1,1,4}, \beta_{1,2,0})^T \ \in \mathbb{R}^{10\times 1}$$

and so is the M_1 function, piecewise defined as in (i). We remark that also in this case we work with function spaces that are piecewise Chebyshev spaces but with different segments. Though, more complicated than in the case of internal bases, the non singularity of the corresponding linear system can still be proven as in [22] and generalizing the ideas in [23].

□

Proposition 3.3. *The boundary function N_2^4 is uniquely identified as $N_2^4 = (M_2)^{'}$ with M_2 the piecewise defined function satisfying*

(i) $M_2(x)|_{[x_0, x_1]} = \sum_{i=0}^{2} \beta_{2,0,i} B_i^3(x - x_0)$ *while* $M_2(x)|_{[x_j, x_{j+1}]} = \sum_{i=0}^{4} \beta_{2,j,i} B_i^5(x - x_j)$, $\quad j = 1, 2, 3$;

(ii) *M_2 and $1 - M_2$ vanish together with their first derivatives at x_0 and with their derivatives up to the third order at x_4, respectively;*

(iii) *is C^3-regular at the internal knots $x_1,\ x_2,\ x_3$.*

Proof. The conditions $(i)-(iii)$ translate into 18 equations equal to the number of the d.o.f. , so that the function M_2, according with the arguments of Proposition 3.1, is uniquely identified. The explicit expression of M_2 requires the solution of the linear system whose equations are coming next with the shorthand notation $M_2^j = M_2(x)|_{[x_j, x_{j+1}]},\ j = 0, \cdots, 3$. Firstly, we consider the requirement in (ii):

$$(M_2^0)^{(k)}(x_0) = 0, \quad k = 0, 1 \quad \Leftrightarrow \beta_{2,0,k} = 0, \quad k = 0, 1, \tag{16}$$

and

$$(1 - M_2^3)^{(k)}(x_4) = 0, \quad k = 0, \cdots, 3 \quad \Leftrightarrow \beta_{2,3,4-k} = 1, \quad k = 0, \cdots, 3. \tag{17}$$

Concerning (iii), at the points $x_1,\ x_2,\ x_3$ we get

$$(M_2^{\ell})^{(k)}(x_{\ell+1}) = (M_2^{\ell+1})^{(k)}(x_{\ell+1}), \quad k = 0, 1, 2, 3 \quad \ell = 0, 1, 2,$$

translating into the linear equations ($\ell = 0$):

$$\sum_{i=0}^{2} \beta_{2,0,i}(B_i^3)^{(k)}(h) = \sum_{i=0}^{4} \beta_{2,1,i}(B_i^5)^{(k)}(0), \qquad k = 0,1,2,3. \tag{18}$$

Similarly when $\ell = 1,2$ (i.e. when dealing with x_2 and x_3 respectively) we compute:

$$\sum_{i=0}^{4} \beta_{2,\ell,i}(B_i^5)^{(k)}(h) = \sum_{i=0}^{4} \beta_{2,\ell+1,i}(B_i^5)^{(k)}(0), \qquad k = 0,1,2,3 \tag{19}$$

Taking into account equations (16) and (17), the 18 equations can be reduced to 12, that uniquely identify the coefficients vector

$$(\beta_{2,0,2}, \beta_{2,1,0}, \cdots, \beta_{2,1,4}, \beta_{2,2,0}, \cdots, \beta_{2,2,4}, \beta_{2,3,0})^T \in \mathbb{R}^{12\times 1}$$

and so is the function M_2 piecewise defined as in (i). As for the case of M_1, we can prove the non singularity of the linear system following [22]. □

In Fig. 2 is described the behaviour of the M_i, $i = 1,2$, and the corresponding boundary functions N_i, $i = 1,2$, for the particular choice of $\alpha = 1/2$.

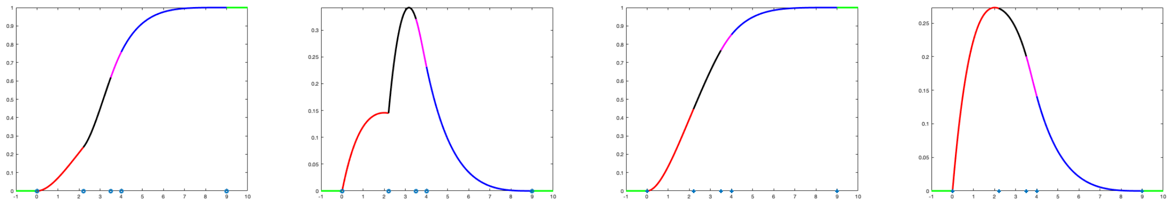

Figure 2: Function M_1 and corresponding N_1 (left), function M_2 and corresponding N_2 (right), for $\alpha = \frac{1}{2}$ and knots denoted by $'*'$.

3.3 Construction of the right boundary bases

The constructive strategy for the right boundary bases N_{N-1}^4 and N_N^4 reflects the construction of the left boundary bases. Firstly, we construct N_{N-1}^4. We require that it has support $[x_{N-3}, x_{N+1}]$ where $b = x_{N+1} < x_{N+2}$. As to the regularity we require it to be $C^2(a,b)$. Then, we construct N_N^4 requiring that it is supported on $[x_{N-2}, x_{N+2}]$ and $C^2(a,b)$. We recall that $\mathbb{E}_3^{'} \equiv \mathbb{E}_2$ while B_i^3, $i = 0,\ldots,2$ and B_i^5, $i = 0,\ldots,4$ are the Bernstein-like basis for $\mathbb{E}_3$ and $\mathbb{E}_5$ related to $[x_j, x_{j+1}]$, respectively.

Proposition 3.4. *The boundary function N_{N-1}^4 is uniquely identified as $N_{N-1}^4 = (M_{N-1})^{'}$ with M_{N-1} the piecewise defined function satisfying*

(i) $M_{N-1}(x)|_{[x_j,x_{j+1}]} = \sum_{i=0}^{4} \beta_{N-1,j,i} B_i^5(x - x_j)$, $j = N-3, N-2, N-1$ *while* $M_{N-1}(x)|_{[x_N,x_{N+1}]} = \sum_{i=0}^{2} \beta_{N-1,N,i} B_i^3(x - x_N)$;

(ii) M_{N-1} *and* $1 - M_{N-1}$ *vanish with their first derivatives at* x_{N+1} *and with their derivatives up to the third order at* x_{N-3}*, respectively;*

(iii) is C^3*-regular at the internal knots* x_{N-2}, x_{N-1}, x_N.

Proof. The proof follows the same line of reasoning as for N_2. □

For the case of N_1 we prove

Proposition 3.5. *The boundary function N_N^4 is uniquely identified as $N_N^4 = (M_N)^{'}$ with M_N the piecewise defined function satisfying*

(i) $M_N(x)|_{[x_j,x_{j+1}]} = \sum_{i=0}^{4} \beta_{N,j,i} B_i^5(x - x_j)$, $\quad j = N-2, N-1$, *while* $M_N(x)|_{[x_j,x_{j+1}]} = \sum_{i=0}^{2} \beta_{N,j,i} B_i^3(x - x_j)$, $j = N, N+1$;

(ii) M_N *and* $1 - M_N$ *vanish with their first derivatives at* x_{N+2} *and with their derivatives up to the third order at* x_{N-2}*, respectively;*

(iii) is C^3*-regular at the internal knots* x_{N-1}, x_N *and* C^1*-regular at* x_{N+1}.

In Figure 3 (from left to right) we report the graphs of the Bernstein-like bases for the spaces $\mathbb{E}_4$ and $\mathbb{E}_5$ respectively, in the case of $\alpha = \frac{1}{2}$.

With the above specified basis function N_ℓ^4, $\ell = 1,\cdots,N$, we use Theorem 2.1 to construct the corresponding natural smoothing exponential-polynomial spline. The following algorithm synthesizes the definition of the described model, that minimizes the functional in (1), shortly referred to as SGBBS, for **S***moothing* **G***eneralized* **B***-spline on* **B***ernestein basis*. When $\lambda = 0$ the procedure provides the interpolating natural $L-$spline of order 4. The model is globally $C^2[a,b]$. Starting from a set of nodes $x := (x_i)_{i=1}^N$ and corresponding values $y := (y_i)_{i=1}^N$, the algorithm provides the coefficients $c := (c_i)_{i=1}^N$ of the representation of

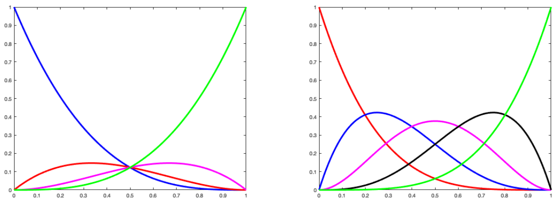

Figure 3: Bernstein-like bases for the space $\mathbb{E}_4$ (left) and $\mathbb{E}_5$ (right) for $\alpha = \frac{1}{2}$

SGBBS defined on $\{x_i\}_{i=1}^N \in [a,b]$, and fitting the data $(x_i, y_i)_{i=1}^N$, in terms of B-splines based on Bernstein bases, N_j, $j = 1, \ldots, N$, just defined in the previous section:

$$s(x) = \sum_{i=1}^{N} c_j N_j(x),$$

Algorithm 1 SGBBS

procedure SGBBS(input: x, y, N, λ, W; output: c)
Definition of matrix Φ: $\Phi_{i,j} = N_j(x_i),\ i,j = 1,\ldots,N$
if $\lambda \neq 0$
    Definition of matrix D: $D_{i,j} = N_j^{(3)}(x_i^+) - N_j^{(3)}(x_i^-),\ i,j = 1,\ldots,N.$
end if
$A = (\Phi + \lambda W\, D)$
solve $Ac = y$
end

4 Numerical experiments

In this section, we describe some numerical results to test the behaviour of the smoothing spline to approximate exponential decay data. The tests were carried out with MATLAB R2018a software on a Intel(R) Core(TM) i5, 1.8 GHz processor.
We fix a set of data, with exponential decay. e.g.:

$$(x_i, \tilde{y}_i)_{i=1}^N, \quad \tilde{y}_i = F(x_i)(1+\epsilon_i), \quad x_i \in [a,b],\ i = 1, ..., N$$

with $a, b \in \mathbb{R}$, F an exponential decaying function and ϵ_i the ith noise component, normally distributed with zero mean and variance σ^2, and we construct the smoothing spline on the nodes $\Delta = \{x_i\}_{i=1}^N$. The model definition requires some settings:

- the parameter α in (4), defining the bases; when unknown, its value has been computed by a *(non-linear) least-squares regression* of the data.
- the regularizing parameter λ in (1); the tests have been made for different λ values; where it is not specified, λ is set in a dynamic way, depending on N and σ as $\lambda = \sigma^2/N$.

The results highlight the behaviour of the presented smoothing exponential-polynomial spline in $[a,b]$ with respect to the number and the distribution of the nodes, to the noise level and to the regularizing parameter. In our tests we consider both uniformly distributed nodes and Halton nodes, that are pseudo-random points but with low discrepancy. An example of the approximation of multi-exponential decay data is also presented. Moreover, some tests compare the approximation furnished on $[a,b]$ with respect to the classical polynomial cubic (smoothing) spline provided by Matlab. The type of data, the error distribution and the function F are reported case by case.

Test 1: fitting of exponential data
Here we test the smoothing properties of our model defined on uniformly distributed nodes, and corresponding values generated by an exponential function $F(x) = e^{-2x}$; we set $N = 36$ and the following parameter values:

$$\alpha = 2;\ a = 0;\ b = 10;\ x_1 = 1\ x_N = 8;$$

moreover we introduce random Gaussian noise with standard deviation $\sigma = 10^{-2}$ and $\sigma = 10^{-4}$, respectively, and present results for $\lambda \in \{1, 10^{-1}, 10^{-2}, \ldots, 10^{-6}\}$. The absolute approximation error on the whole interval $[x_1, x_N]$ is estimated on 141 evaluation points (uniformly distributed). Figure 4 gives the data smoothing and corresponding *absolute error* at the nodes, when the smoothing parameter increases, so regularizing the model fitting the data. The table gives the 2−norm of the absolute error at the node locations, $E = \|\tilde{s} - \tilde{y}\|_2$, with $\tilde{s} = (s(x_i))_{i=1}^N$ and $\tilde{y} = (\tilde{y}_i)_{i=1}^N$:

$E = \|\tilde{s} - \tilde{y}\|_2$

λ	$\sigma = 10^{-2}$	$\sigma = 10^{-4}$
1.0	$4.516930581844061e-02$	$3.832681277491880e-02$
$1.0e-01$	$4.027549905107795e-02$	$2.467561663031034e-02$
$1.0e-02$	$4.614069240955995e-02$	$1.041857490342722e-02$
$1.0e-03$	$5.983259079782639e-02$	$3.378769693977035e-03$
$1.0e-04$	$7.658946947711796e-02$	$1.083192199742291e-03$
$1.0e-05$	$8.412049742009961e-02$	$8.616015971733528e-04$
$1.0e-06$	$8.519368399925661e-02$	$8.537732205069357e-04$

The results confirm the smoothing behaviour of the model, depending on λ; particularly, the fidelity to the data converges to the order of magnitude of the error assumed on them, when λ decreases.

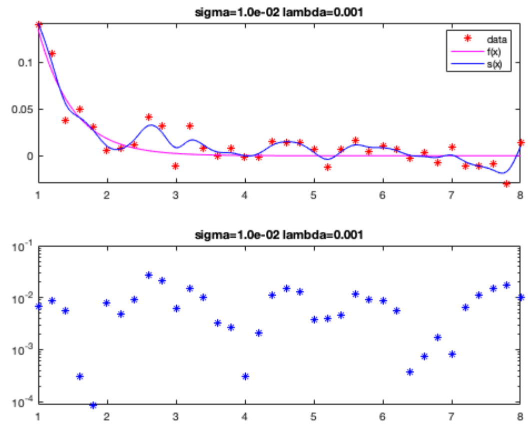

(a) $\lambda = 0.001$

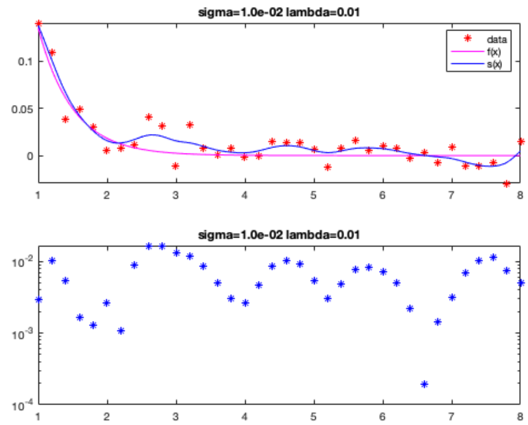

(b) $\lambda = 0.01$

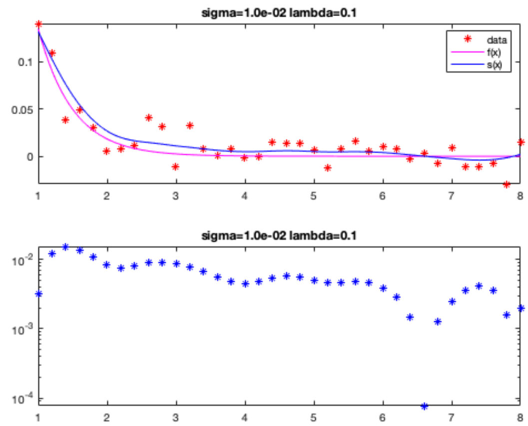

(c) $\lambda = 0.1$

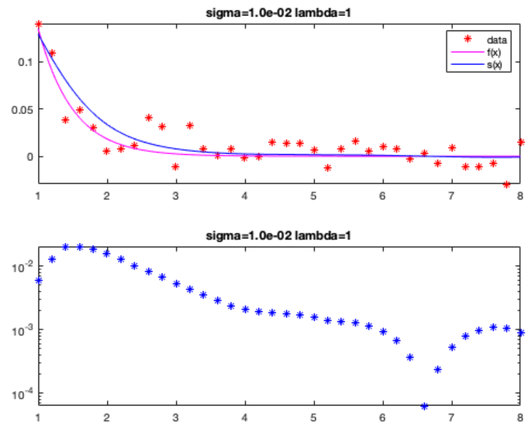

(d) $\lambda = 1$

Figure 4: Smoothing splines for uniform distributed nodes (upper graphs) and corresponding absolute errors at the nodes (lower graphs), when the smoothing parameter λ increases, for $F(x) = e^{-2x}$ and $\sigma = 10^{-2}$.

Fig. 5 shows the same results for data generated by the exponential function $F(x) = e^{-x/10}$ less quickly decreasing towards zero. In this case the numerical experiments reveal an edge effect, i.e. most of the error is localized near the first and last few knots where an oscillating behaviour of the spline model is observed. Though expected, probably due to the construction of "boundary" bases, further investigation of this issue is planned in near future work.

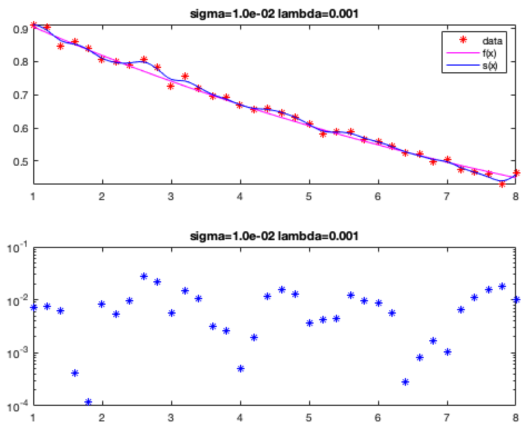

(a) $\lambda = 0.001$

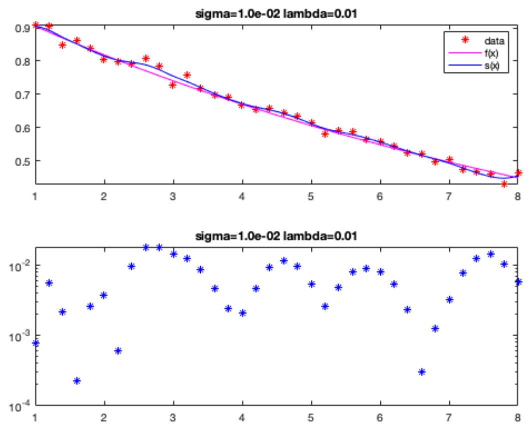

(b) $\lambda = 0.01$

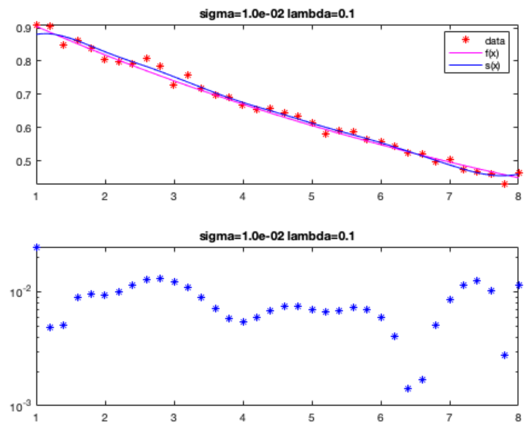

(c) $\lambda = 0.1$

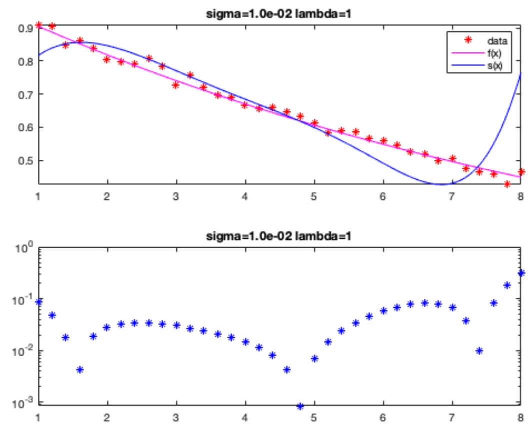

(d) $\lambda = 1$

Figure 5: Smoothing splines for uniform distributed nodes (upper graphs) and corresponding absolute errors at the nodes (lower graphs), when the smoothing parameter λ increases, for $F(x) = e^{-x/10}$ and $\sigma = 10^{-2}$.

Test 2: fitting of multi-exponential decay data
Here we test the model on a dataset of non uniformly distributed data, generated by a sum of exponential functions, $F(x) = 4e^{-2x} + 2e^{-4x}$. Specifically we assume $N = 20$ Halton points in $(0, 1)$ and shifted in (a, b), with $a = 1.5$ and $b = 20$. The parameter α is set as $\alpha = 2$; it has been defined by a (non linear) regression of the data, using the MATLAB function `nlinfit` that, given an initial guess, a generic function, e.g.

$$g(x) = a_1\, x\, e^{-\alpha x} + a_2\, e^{-\alpha x} \in \mathbb{E}_2$$

and given a dataset, furnishes the best parameters in order to fit the data. The relative error at the nodes is of order $\sigma = 10^{-2}$ and λ is dynamically assigned by $\lambda = \sigma^2/N$. Fig. 6a show the nodes distribution. Figure 6b shows the smoothing spline and the corresponding absolute error at the nodes, when $\sigma = 10^{-2}$.
Furthermore, in this test we compare our model with the cubic smoothing spline s_3, implemented in MATLAB by the function `csaps`, minimizing the functional

$$p \sum_j W_j |\tilde{y}_j - s_3(x_j)|^2 + (1-p) \int_{x_1}^{x_N} |D^2 s_3|^2.$$

Figure 7 shows a comparison between the two models, for fixed $\lambda = 0.01$ and $p = 1/(\lambda + 1)$ respectively, and corresponding absolute errors at the nodes. In figure 8 we report a comparison between the two *interpolating models* (i.e. fixed $\lambda = 0$ and $p = 1$ respectively) and the absolute error estimated on a fine grid of evaluation points in $[x_1, x_N]$. In both cases we observe a best fitting of the exponential decay furnished by our model with respect to the polynomial one.

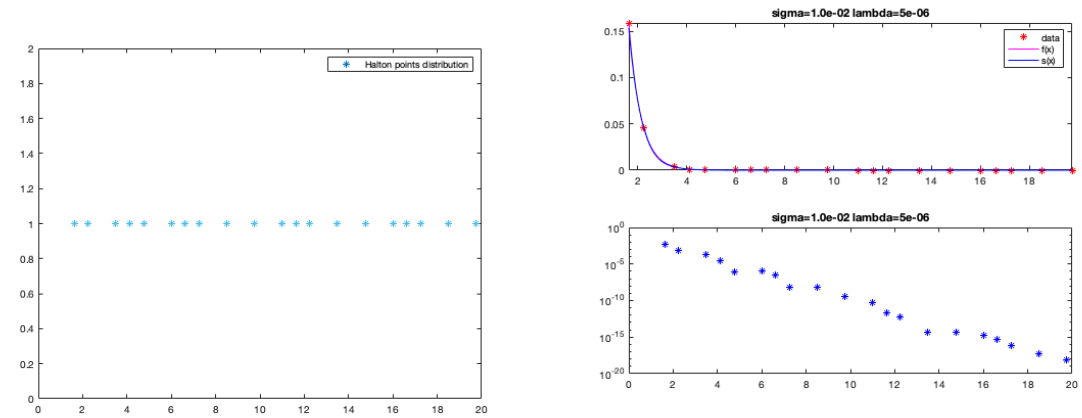

(a) Halton points generated in $(0, 1)$ and shifted in $[a, b]$, with $N = 20$, $a = 1.5$ and $b = 20$.

(b) Smoothing spline for $N = 20$ Halton points (upper graph) and corresponding absolute error at the nodes (lower graph), $\sigma = 10^{-2}$, $F(x) = 4e^{-2x} + 2e^{-4x}$, $\alpha = 2$.

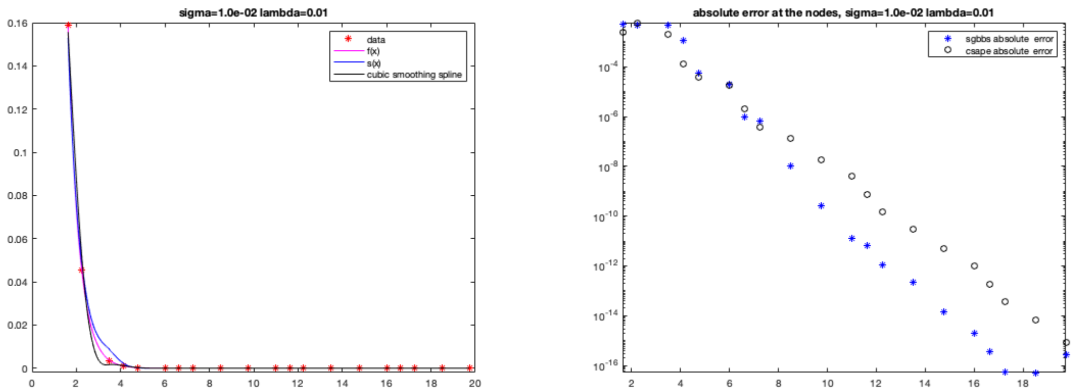

(a) s vs s_3

(b) s vs s_3: absolute error at the nodes

Figure 7: Smoothing sgbbs vs cubic spline at $N = 20$ Halton points, $\sigma = 10^{-2}$, $F(x) = 4e^{-2x} + 2e^{-4x}$, $\alpha = 2$, $\lambda = 0.01$.

Test 3: asymptotic model behaviour
In this test we compare the *asymptotic* behaviour of our model with the one of the cubic spline, referring to the behaviour outside the nodes. To this end we consider the interpolating models, by setting $\sigma = 0$ and $\lambda = 0$; moreover we assume 50 nodes uniformly

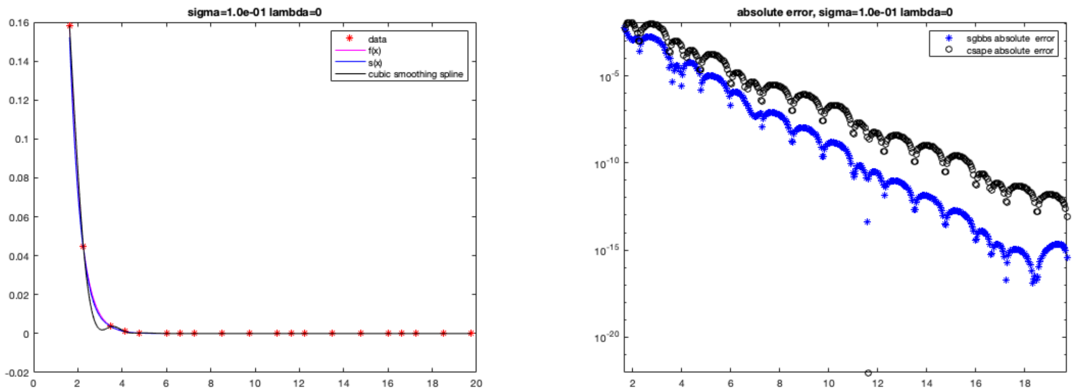

(a) s vs s_3 **(b)** s vs s_3: absolute error at 141 evaluation points in $[x_1, x_N]$

Figure 8: Smoothing sgbbs vs cubic spline at $N = 20$ Halton points, $\sigma = 10^{-2}$, $F(x) = 4e^{-2x} + 2e^{-4x}$, $\alpha = 2$, $\lambda = 0$.

distributed in $[a, b] = [0, 30]$, with $x_1 = 0.5$, $x_N = 25$; finally we set $y_i = F(x_i)$, $i = 1, \dots, N$ with $F(x) = e^{-x}x^2$ and $\alpha = 1$. Fig. 9 displays the exponential-polynomial spline behaviour and a comparison with the polynomial behaviour in $(x_N, b]$. The comparison confirms the better fitting of our model in describing the (multi)exponential decay of the data.

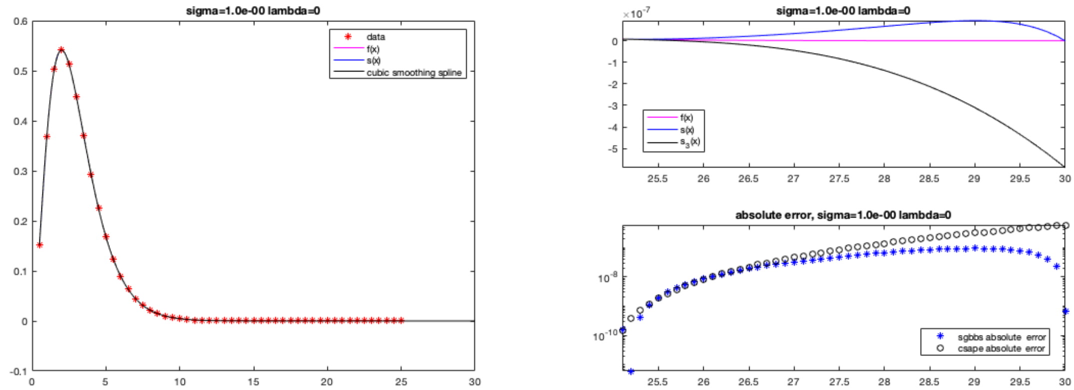

(a) Smoothing spline vs polynomial cubic spline **(b)** s vs s_3 and corresponding absolute errors in $(x_N, b]$.

Figure 9: Smoothing exponential-polynomial spline vs polynomial cubic spline on 50 nodes uniformly distributed in $[a, b] = [0, 30]$, with $x_1 = 0.5$, $x_N = 25$, $y_i = F(x_i)$, $i = 1, \dots, N$, $F(x) = e^{-x}x^2$ and $\alpha = 1$ (left). Comparison with the polynomial cubic spline outside the nodes interval (right).

Similar results have been obtained by setting $F(x) = e^{-x/4}cos(x)$ and $\alpha = 0.25$, on a dataset of 30 nodes uniformly distributed in $[a, b] = [0, 20]$, with $x_1 = 0.5$, $x_N = 15$ (fig. 10).

5 Conclusions and future work

In this work, we propose a natural smoothing exponential-polynomial spline to model data that exponentially decay toward zero. This is a scenario found in many applications. The definition is made through local bases enjoying several properties of polynomial B-splines locally expressed in terms of Bernstein(-like) local bases, granting well conditioning of the linear system for the spline representation. Some insights about the boundary behaviour and a detailed analysis of the sensitivity of the model are under investigation and will be object of future studies.

6 Acknowledgement

Special thanks to the INdAM Research group GNCS and to the Research ITalian network on Approximation (RITA) group fostering collaboration and progress in research. The authors would like to thank Gerardo Toraldo and Carolina Beccari for useful discussion.

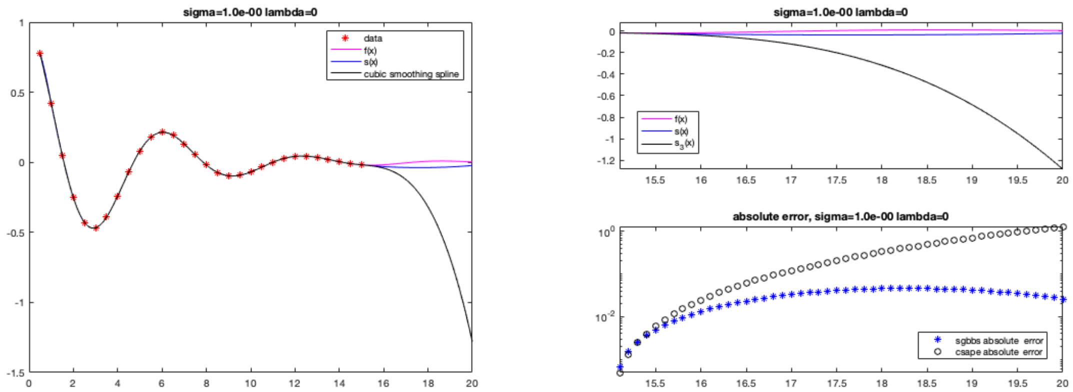

(a) Smoothing spline vs polynomial cubic spline **(b)** s vs s_3 and corresponding absolute errors in $(x_N, b]$.

Figure 10: Smoothing exponential-polynomial spline vs polynomial cubic spline on 30 nodes uniformly distributed in $[a, b] = [0, 20]$, with $x_1 = 0.5$, $x_N = 15$, $y_i = F(x_i)$, $i = 1, \dots, N$, $F(x) = e^{-x/4} cos(x)$ and $\alpha = 0.25$ (left). Comparison with the polynomial cubic spline outside the nodes interval (right).

A Construction of Bernstein-like bases

Following [17], the Bernstein-like bases are defined as follows:

Definition A1. Given $B_0, \dots, B_n \in \mathbb{E}_{n+1}$, $(n+1)$—dimensional space $\mathbb{E}_{n+1} \subset C^n(I)$, we say that $(B_0, \dots, B_n)$ is a Bernstein-like basis of $\mathbb{E}_{n+1}$ relative to (c, d) when the following two properties are satisfied:

(1) for $k = 0, ..., n$, B_k vanishes exactly k times at c, and exactly $(n-k)$ times at d;

(2) for $k = 0, ..., n$, B_k is positive on $]c, d[$.

In the following, we refer to a generic interval $[0, h]$ from which the corresponding bases on a subinterval $[x_j, x_{j+1}]$ will be obtained by the linear transformation

$$x \in [x_j, x_{j+1}] \to z \in [0, h], \quad z = x - x_j.$$

This allow to omit the subscript j referring to $[x_j, x_{j+1}]$ in the names of the Bernstein(-like) functions.

A.1 Bernstein basis for the space $\mathbb{E}_2$

In this section we build the Bernstein-like two dimensional basis to represent the border GB-splines outside the nodes. For simplicity of notation, in this one and the next subsection we set $\tilde{B}_i := B^2_{i,j}$, $i = 0, 1$ and $B_i := B^3_{i,j}$, $i = 0, 1, 2$.
Following [16] (see also [24]), we consider the BVP

$$\begin{cases} u'' + 2\alpha\, u' + \alpha^2\, u = 0, & u \in H^2[a, b], \\ u(0) = 0, \\ u^{'}(0) = 1. \end{cases}$$

The unique solution of the above boundary value problem is

$$s(x) = x\, e^{-\alpha\, x} \tag{20}$$

and the two Bernstein basis related to $[0, h]$ for the 2-dimensional space $\mathbb{E}_2 := span\{e^{-\alpha x},\ x\, e^{-\alpha x}\}$, are:

$$\tilde{B}_1(x) := \frac{s(x)}{s(h)}, \quad \tilde{B}_0(x) := \tilde{B}_1(h - x), \tag{21}$$

that assume the values in the following:

Proposition A.1. *With the shorthand notation*

$$d^h_0 = \frac{1}{s(h)}, \quad d^h_1 = \frac{s'(h)}{s(h)}, \quad d^h_2 = \frac{s''(h)}{s(h)}$$

it is simple to check that

$$\begin{cases} \tilde{B}_0(0) = 1 \\ \tilde{B}_0(h) = 0 \end{cases} \quad \begin{cases} \tilde{B}^{'}_0(0) = -d^h_1 \\ \tilde{B}^{'}_0(h) = -d^h_0 \end{cases} \quad \begin{cases} \tilde{B}^{''}_0(0) = d^h_2 \\ \tilde{B}^{''}_0(h) = -2\alpha d^h_0 \end{cases}$$

$$\begin{cases} \tilde{B}_1(0) = 0 \\ \tilde{B}_1(h) = 1 \end{cases} \quad \begin{cases} \tilde{B}^{'}_1(0) = d^h_0 \\ \tilde{B}^{'}_1(h) = d^h_1 \end{cases} \quad \begin{cases} \tilde{B}^{''}_1(0) = -2\alpha d^h_0 \\ \tilde{B}^{''}_1(h) = d^h_2 \end{cases}$$

A.2 Bernstein basis for the space $\mathbb{E}_3$

As announced we need an auxiliary Bernstein-basis for the space $\mathbb{E}_3 := span\{1,\ e^{-\alpha x},\ x\,e^{-\alpha x}\}$. According to [16] this basis $\{B_i(x)\}_{i=0,\cdots,2}$, related to $(0,h)$ can be constructed from the $\tilde{B}_i(x),\ i=0,1$ of $\mathbb{E}_2$ defined in (21) as follows:

$$\begin{aligned} B_2(x) &= \frac{\int_0^x \tilde{B}_1(t)dt}{\int_0^h \tilde{B}_1(t)dt} = \frac{\int_0^x s(t)dt}{\int_0^h s(t)dt} \\ B_1(x) &= \frac{\int_0^x \tilde{B}_0(t)dt}{\int_0^h \tilde{B}_0(t)dt} - \frac{\int_0^x \tilde{B}_1(t)dt}{\int_0^h \tilde{B}_1(t)dt} = \frac{\int_{h-x}^h s(t)dt}{\int_0^h s(t)dt} - B_2(x) \\ B_0(x) &= 1 - \frac{\int_0^x \tilde{B}_0(t)dt}{\int_0^h \tilde{B}_0(t)dt} = 1-(B_1(x)+B_2(x)). \end{aligned} \tag{22}$$

satisfying the following:

Proposition A.2. *The basis functions $B_i(x),\ i=0,\cdots,2$ satisfy*

$$\sum_{i=0}^{2} B_i(x) = 1 \quad \textit{for all} \quad x\in[0,h].$$

As to the function and derivative values we have:

$$\begin{cases} B_0(0)=1 \\ B_0(h)=0 \end{cases} \quad \begin{cases} B_0^{'}(0)=-1/K_2^{0,h} \\ B_0^{'}(h)=0 \end{cases} \quad \begin{cases} B_0^{''}(0)=d_1^h/K_2^{0,h} \\ B_0^{''}(h)=d_0^h/K_2^{0,h} \end{cases} \quad \begin{cases} B_0^{'''}(0)=-d_2^h/K_2^{0,h} \\ B_0^{'''}(h)=2\alpha d_0^h/K_2^{0,h} \end{cases}$$

$$\begin{cases} B_1(0)=0 \\ B_1(h)=0 \end{cases} \quad \begin{cases} B_1^{'}(0)=1/K_2^{0,h} \\ B_1^{'}(h)=-1/K_2^{1,h} \end{cases} \quad \begin{cases} B_1^{''}(0)=-d_1^h/K_2^{0,h}-d_0^h/K_2^{1,h} \\ B_1^{''}(h)=-d_0^h/K_2^{0,h}-d_1^h/K_2^{1,h} \end{cases} \quad \begin{cases} B_1^{'''}(0)=d_2^h/K_2^{0,h}+2\alpha d_0^h/K_2^{1,h} \\ B_1^{'''}(h)=-2\alpha d_0^h/K_2^{0,h}-d_2^h/K_2^{1,h} \end{cases}$$

$$\begin{cases} B_2(0)=0 \\ B_2(h)=1 \end{cases} \quad \begin{cases} B_2^{'}(0)=0 \\ B_2^{'}(h)=1/K_2^{1,h} \end{cases} \quad \begin{cases} B_2^{''}(0)=d_0^h/K_2^{1,h} \\ B_2^{''}(h)=d_1^h/K_2^{1,h} \end{cases} \quad \begin{cases} B_2^{'''}(0)=-2\alpha d_0^h/K_2^{1,h} \\ B_2^{'''}(h)=d_2^h/K_2^{1,h} \end{cases}$$

with $K_2^{i,h} = \int_0^h \tilde{B}_i(t)dt$ where the subscript 2 refers to $\mathbb{E}_2$.

A.3 Bernstein basis for the space $\mathbb{E}_4$

In a similar way to what has just been described, we define a Bernstein-like basis on the interval $[0,h]$ for the space $\mathbb{E}_4 = span\{e^{\alpha x},\ x\,e^{\alpha x},\ e^{-\alpha x},\ x\,e^{-\alpha x}\}$. Set $\tilde{B}_i := B^4_{i,j},\ i=0,\dots,3$ and $B_i := B^5_{i,j},\ i=0,\dots,4$, we consider the BVP:

$$\begin{cases} v^{(iv)} - 2\alpha^2 v^{''} + \alpha^4 v = 0 \\ v^{(j)}(0)=0, \quad j=0,1,2, \\ v^{'''}(0)=1. \end{cases}$$

whose only solution is the following:

$$s(x) = \frac{1}{4\alpha^2}\left[(x-\frac{1}{\alpha})e^{\alpha x} + (x+\frac{1}{\alpha})e^{-\alpha x}\right], \tag{23}$$

Setting $H := ss^{''} - (s^{'})^2$ the determinant of the Wronskian matrix $W(s,s^{'},s^{''}) := \begin{pmatrix} s & s^{'} \\ s^{'} & s^{''} \end{pmatrix}$, the four Bernstein-like functions in $[0,h]$ for the symmetry property are

$$\tilde{B}_3(x) := \frac{s(x)}{s(h)}, \quad \tilde{B}_0(x) := \tilde{B}_3(h-x), \tag{24}$$

and

$$\tilde{B}_2(x) := \frac{s^{'}(h)s(x)-s(h)s^{'}(x)}{H(h)}, \quad \tilde{B}_1(x) := \tilde{B}_2(h-x). \tag{25}$$

enjoying the following properties:

Proposition A.3. *With the shorthand notation*

$$d_0^h = \frac{s(h)}{H(h)}, \quad d_1^h = \frac{s'(h)}{s(h)}, \quad d_2^h = \frac{s''(h)}{s(h)},$$

and

$$w_1^h = \frac{(s'(h))^2 - s(h)s''(h)}{H(h)}, \quad w_2^h = \frac{s'(h)s''(h)-s(h)s'''(h)}{H(h)},$$

it is simple to check that

$$\begin{cases}\tilde{B}_0(0)=1,\\ \tilde{B}_0(h)=0\end{cases}\quad \begin{cases}\tilde{B}_0'(0)=-d_1^h,\\ \tilde{B}_0'(h)=0\end{cases}\quad \begin{cases}\tilde{B}_0''(0)=d_2^h,\\ \tilde{B}_0''(h)=0\end{cases}$$

$$\begin{cases}\tilde{B}_1(0)=0,\\ \tilde{B}_1(h)=0\end{cases}\quad \begin{cases}\tilde{B}_1'(0)=-w_1^h,\\ \tilde{B}_1'(h)=0\end{cases}\quad \begin{cases}\tilde{B}_1''(0)=w_2^h,\\ \tilde{B}_1''(h)=-d_0^h\end{cases}$$

$$\begin{cases}\tilde{B}_2(0)=0,\\ \tilde{B}_2(h)=0\end{cases}\quad \begin{cases}\tilde{B}_2'(0)=0,\\ \tilde{B}_2'(h)=w_1^h\end{cases}\quad \begin{cases}\tilde{B}_2''(0)=-d_0^h,\\ \tilde{B}_2''(h)=w_2^h\end{cases}$$

$$\begin{cases}\tilde{B}_3(0)=0,\\ \tilde{B}_3(h)=1\end{cases}\quad \begin{cases}\tilde{B}_3'(0)=0,\\ \tilde{B}_3'(h)=d_1^h\end{cases}\quad \begin{cases}\tilde{B}_3''(0)=0,\\ \tilde{B}_3''(h)=d_2^h\end{cases}$$

Hence, every function of type

$$s(x)=\sum_{i=0}^{3}\tilde{\gamma}_i\tilde{B}_i(x),\quad x\in[0,h] \tag{26}$$

satisfies

$$\begin{cases}s(0)=\tilde{\gamma}_0\\ s(h)=\tilde{\gamma}_3\end{cases}\quad \begin{cases}s'(0)=-d_1^h\tilde{\gamma}_0-w_1^h\tilde{\gamma}_1\\ s'(h)=w_1^h\tilde{\gamma}_2+d_1^h\tilde{\gamma}_3\end{cases}\quad \begin{cases}s''(0)=d_2^h\tilde{\gamma}_0+w_h^2\tilde{\gamma}_1-d_0^h\tilde{\gamma}_2\\ s''(h)=-d_0^h\tilde{\gamma}_1+w_2^h\tilde{\gamma}_2+d_2^h\tilde{\gamma}_3\end{cases} \tag{27}$$

A.4 Bernstein basis for the space $\mathbb{E}_5$

We continue by consider the problem of constructing a Bernstein-like basis on the interval $[0,h]$ for the space $\mathbb{E}_5$ based on the Bernstein-like basis on the interval $[0,h]$ for the space $\mathbb{E}_4$. According to [16] the Bernstein basis $B_i(x),\ i=0,\cdots,4$ of $\mathbb{E}_5$ related to $(0,h)$ can be constructed from the $\tilde{B}_i(x),\ i=0,\cdots,3$ of $\mathbb{E}_4$ defined in (24) and (25) as follows

$$\begin{aligned} B_0(x) &= 1-\frac{\int_0^x\tilde{B}_0(t)dt}{\int_0^h\tilde{B}_0(t)dt},\quad B_4(x)=\frac{\int_0^x\tilde{B}_3(t)dt}{\int_0^h\tilde{B}_3(t)dt},\\ B_i(x) &= \frac{\int_0^x\tilde{B}_{i-1}(t)dt}{\int_0^h\tilde{B}_{i-1}(t)dt}-\frac{\int_0^x\tilde{B}_i(t)dt}{\int_0^h\tilde{B}_i(t)dt},\quad i=1,2,3,\end{aligned} \tag{28}$$

The next Proposition investigates the corresponding properties. The proof is just a computation.

Proposition A.4. *The basis functions $B_i(x),\ i=0,\cdots,4$ satisfy*

$$\sum_{i=0}^{4}B_i(x)=1\quad \textit{for all}\quad x\in[0,h].$$

As to the function and derivative values we have:

$$\begin{cases}B_0(0)=1,\\ B_0(h)=0\end{cases}\quad \begin{cases}B_0'(0)=-1/K_4^{0,h},\\ B_0'(h)=0\end{cases}\quad \begin{cases}B_0''(0)=d_1^h/K_4^{0,h},\\ B_0''(h)=0\end{cases}\quad \begin{cases}B_0'''(0)=-d_2^h/K_4^{0,h},\\ B_0'''(h)=0\end{cases}$$

$$\begin{cases}B_1(0)=0,\\ B_1(h)=0\end{cases}\quad \begin{cases}B_1'(0)=1/K_4^{0,h},\\ B_1'(h)=0\end{cases}\quad \begin{cases}B_1''(0)=-d_1^h/K_4^{0,h}+w_1^h/K_4^{1,h},\\ B_1''(h)=0\end{cases}\quad \begin{cases}B_1'''(0)=d_2^h/K_4^{0,h}-w_2^h/K_4^{1,h},\\ B_1'''(h)=d_0^h/K_4^{1,h}\end{cases}$$

$$\begin{cases}B_2(0)=0,\\ B_2(h)=0\end{cases}\quad \begin{cases}B_2'(0)=0,\\ B_2'(h)=0\end{cases}\quad \begin{cases}B_2''(0)=-w_1^h/K_4^{1,h},\\ B_2''(h)=-w_1^h/K_4^{2,h}\end{cases}\quad \begin{cases}B_2'''(0)=w_2^h/K_4^{1,h}+d_0^h/K_4^{2,h},\\ B_2'''(h)=-d_0^h/K_4^{1,h}-w_2^h/K_4^{2,h}\end{cases}$$

$$\begin{cases}B_3(0)=0,\\ B_3(h)=0\end{cases}\quad \begin{cases}B_3'(0)=0,\\ B_3'(h)=-1/K_4^{3,h}\end{cases}\quad \begin{cases}B_3''(0)=0,\\ B_3''(h)=w_1^h/K_4^{2,h}-d_1^h/K_4^{3,h}\end{cases}\quad \begin{cases}B_3'''(0)=-d_0^h/K_4^{2,h},\\ B_3'''(h)=w_2^h/K_4^{2,h}-d_2^h/K_4^{3,h}\end{cases}$$

$$\begin{cases}B_4(0)=0,\\ B_4(h)=1\end{cases}\quad \begin{cases}B_4'(0)=0,\\ B_4'(h)=1/K_4^{3,h}\end{cases}\quad \begin{cases}B_4''(0)=0,\\ B_4''(h)=d_1^h/K_4^{3,h}\end{cases}\quad \begin{cases}B_4'''(0)=0,\\ B_4'''(h)=d_2^h/K_4^{3,h}\end{cases}$$

with $K_4^{i,h}=\int_0^h\tilde{B}_i(t)dt,\ i=0,1,2,3.$

References

[1] F. Babiloni, C. Babiloni, F. Carducci, L. Fattorini, P. Onorati, A. Urbano, Spline laplacian estimate of eeg potentials over a realistic magnetic resonance-constructed scalp surface model., Electroencephalography and clinical neurophysiology 98 4 (1996) 363–73.

[2] E. R. Brown, J. G. Ibrahim, V. D. Gruttola, A flexible b-spline model for multiple longitudinal biomarkers and survival, Biometrics 61 (1) (2005) 64–73.

[3] P. Hancock, M. Hutchinson, Spatial interpolation of large climate data sets using bivariate thin plate smoothing splines, Environmental Modelling & Software 21 (12) (2006) 1684 – 1694.

[4] A. Arcioni, R. Tarroni, C. Zannoni, Global target analysis of fluorescence depolarization in model membranes using exponential splines, J. Chem. Soc. Faraday Trans. 89 (1993) 2815–2822.

[5] P. Barone, A. Ramponi, G. Sebastiani, On the numerical inversion of the Laplace transform for nuclear magnetic resonance relaxometry, Inverse Problems 17 (1) (2001) 77–94.

[6] L. D'Amore, V. Mele, R. Campagna, Quality assurance of Gaver's formula for multi-precision Laplace transform inversion in real case, Inverse Problems in Science and Engineering 26 (4) (2018) 553–580.

[7] M. R. Naeeni, R. Campagna, M. Eskandari-Ghadi, A. A. Ardalan, Performance comparison of numerical inversion methods for Laplace and Hankel integral transforms in engineering problems, Applied Mathematics and Computation 250 (2015) 759 – 775.

[8] R. Campagna, L. D'Amore, A. Murli, An efficient algorithm for regularization of Laplace transform inversion in real case, Journal of Computational and Applied Mathematics 210 (1) (2007) 84 – 98, proceedings of the Numerical Analysis Conference 2005.

[9] R. Mao, J. Tang, B. Swanson, Relaxation time spectrum of hydrogels by CONTIN analysis, Journal of Food Science 65 (3) (2000) 374–381.

[10] L. D'Amore, R. Campagna, V. Mele, A. Murli, Algorithm 946: Reliadiff–a c++ software package for real Laplace Transform Inversion based on Algorithmic Differentiation, ACM Trans. Math. Softw. 40 (4) (2014) 31:1–31:20.

[11] L. D'Amore, R. Campagna, V. Mele, A. Murli, Relative. An Ansi C90 software package for the Real Laplace Transform Inversion, Numerical Algorithms 63 (1) (2013) 187–211.

[12] H. Weber, Fourier, Laplace and other Integral Transforms, https://www.cs.hs-rm.de/~weber/lapinv/lapinv.htm (2019).

[13] L. D'Amore, R. Campagna, A. Galletti, L. Marcellino, A. Murli, A smoothing spline that approximates Laplace transform functions only known on measurements on the real axis, Inverse Problems 28 (2) (2012) 025007.

[14] T. Lyche, L. L. Schumaker, Computation of smoothing and interpolating natural splines via local bases, SIAM Journal on Numerical Analysis 10 (6) (1973) 1027–1038.

[15] S. Seatzu, Un metodo per la costruzione di smoothing splines naturali mono e bidimensionali, CALCOLO 12 (3) (1975) 259–273.

[16] M. Brilleaud, M.-L. Mazure, Mixed hyperbolic/trigonometric spaces for design, Computers & Mathematics with Applications 64 (2012) 2459–2477.

[17] C. V. Beccari, G. Casciola, M.-L. Mazure, Design or not design? A numerical characterisation for piecewise Chebyshevian splines, Numerical Algorithms (2018) 1 – 31.

[18] C. Conti, M. Cotronei, L. Romani, Beyond b-splines: exponential pseudo-splines and subdivision schemes reproducing exponential polynomials, Dolomites Research Notes on Approximation 10 (2017) 31–42.

[19] L. Schumaker, Spline Functions: Basic Theory, 3rd Edition, Cambridge Mathematical Library, Cambridge University Press, 2007.

[20] C. V. Beccari, G. Casciola, M.-L. Mazure, Piecewise Extended Chebyshev Spaces, Appl. Math. Comput. 296 (C) (2017) 239–256.

[21] M. L. Mazure, Constructing totally positive piecewise chebyshevian b-spline bases, Journal of Computational and Applied Mathematics 342 (2018) 550 – 586.

[22] B. Buchwald, G. Mühlbach, Construction of b-splines for generalized spline spaces generated from local ect-systems, Journal of Computational and Applied Mathematics 159 (2) (2003) 249 – 267.

[23] C. Beccari, G. Casciola, S. Morigi, On multi-degree splines, Computer Aided Geometric Design 58 (2017) 8–23.

[24] E. Mainar, J. M. Peña, Optimal bases for a class of mixed spaces and their associated spline spaces, Computers & Mathematics with Applications 59 (4) (2010) 1509 – 1523.